ceramics

Article

Deliberate Surface Treatment of Zirconium Dioxide with Abrasive Brushing Tools

Anton Hoyer [1,*] and Eckart Uhlmann [1,2]

[1] Institute for Machine Tools and Factory Management (IWF), Technische Universität Berlin, Pascalstr. 8-9, 10587 Berlin, Germany
[2] Fraunhofer Institute for Production Systems and Design Technology IPK, Technische Universität Berlin, Pascalstr. 8-9, 10587 Berlin, Germany
* Correspondence: hoyer@iwf.tu-berlin.de; Tel.: +49-30-314-22781

Abstract: Brushing with bonded abrasives is a flexible finishing process used to reduce the roughness of technical surfaces. Although industrially widespread, especially for the finishing of metallic surfaces, insufficient knowledge of the motion, the material removal, and the wear behavior of the abrasive filaments complicates predictions of the work result. In particular, the reliable finishing of ceramics with bonded diamond grains proves difficult due to increased material removal rates, quickly leading to undesirable changes in the workpiece geometry. Based on technological investigations with abrasive brushing tools, this article provides insights into the surface finishing of zirconium dioxide with a focus on finding compromises between reduction in the surface roughness and alteration of the workpiece shape.

Keywords: brushing; abrasive brushing; bonded abrasives; surface finishing; Mg-PSZ; ZrO_2

check for updates

Citation: Hoyer, A.; Uhlmann, E. Deliberate Surface Treatment of Zirconium Dioxide with Abrasive Brushing Tools. *Ceramics* **2022**, *5*, 883–900. https://doi.org/10.3390/ceramics5040064

Academic Editor: Gilbert Fantozzi

Received: 30 September 2022
Accepted: 21 October 2022
Published: 1 November 2022

1. Introduction

Brushing with bonded abrasives is a manufacturing process industrially used for the deburring and the rounding of workpiece edges as well as the finishing of technical surfaces, specifically with the goal of decreasing the surface roughness without affecting the workpiece geometry [1–5]. Crucial for the process are its flexible brushing tools, which normally consist of a multitude of abrasive filaments attached to an epoxy brush body, Figure 1. The abrasive filaments are composed of an extruded polymer matrix, typically polyamide 6.12, and bonded abrasive grains, typically silicon carbide (SiC) or aluminum oxide (Al_2O_3). Harder abrasive materials, such as diamond or cubic boron nitride (cBN), may be used to extend the range of machinable materials, particularly in regard to finishing ceramic workpieces [6–9].

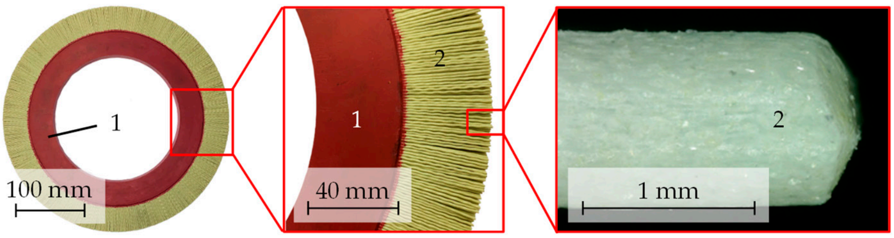

Figure 1. Layout of a round brush, consisting of a brush body (1) and abrasive filaments (2).

The high flexibility of the abrasive filaments enables even ordinarily shaped tools to adapt to complexly shaped workpieces by compensating for small inaccuracies of the tool or the workpiece geometry, as well as of tool trajectories or the machine system. The multidirectional motion and cutting patterns of the abrasive filaments yield surfaces of high quality and minimal geometrical deviations, ideally removing only roughness peaks while retaining roughness valleys for enhanced lubrication properties. Further benefits are low process temperatures as well as the potential to utilize pre-existing grinding or milling machine systems [1,3–5].

However, the full potential of brushing processes remains largely unused due to the insufficiently understood motion, material removal, and wear behaviors of the abrasive filaments, making predictions for process results difficult, therefore causing industrial applications to be largely based on experiential values [3–5]. Several studies on the brushing of metallic surfaces confirm a strong correlation between contact forces and the work result because high contact forces lead to deep penetration of the workpiece material by the abrasive grains [1–5,10].

In contrast, studies on the brushing of oxide ceramics are few, most notably indicating a lower process reliability compared to the brushing of metals: on the one hand, finishing ceramics necessitates the use of diamond grains due to the high hardness of ceramics in general. This leads to large material removal rates Q_w and subsequently to large workpiece geometry deviations [7], whereas steel surfaces may be brushed successively without distinctly changing the workpiece geometry, but merely reducing the surface roughness until a tool-specific threshold roughness is reached [4,5]. On the other hand, the low thermal conductivity of ceramic materials, particularly when compared with previously investigated metals, also increases the likelihood of tool wear. This holds true especially for dry brushing processes without the use of cooling lubricant, at worst melting the polymer matrix of the abrasive filaments, resulting in irreversible tool damage [4].

As for potential applications, dental prosthetics typically require very low surface roughness in order to prevent bacteria growth, peri-implant inflammation, and long-term bone loss [11–13], yet may allow for higher shape deviations than an application exposed to high frictional forces, such as artificial hip joints or roller bearings, the latter of which would require the absence of roughness peaks but the presence of roughness valleys to retain lubricating fluids. Consequently, just as wide as the potential application range of ceramics needs to be its range of deliberate surface treatments, a task for which brushing tools with bonded abrasives proved highly suitable.

Thus, the aim of this article is to gain a better understanding of the dry finishing of ceramic surfaces using brushing tools with bonded abrasives. This is achieved through technological investigations with different tool specifications and process parameter combinations, evaluating the work result on the basis of surface roughness and topography measurements.

2. Materials and Methods

The material investigated within the scope of this article was zirconium dioxide of type Frialit FZM, manufactured by Friatec GmbH, Mannheim, Germany, and chosen for its comparably ductile machining properties. The material was partially stabilized with magnesium oxide (Mg-PSZ) to prevent tetragonal to monoclinic phase transformation, which increases the fracture toughness [14,15]. Compared to the more common variant stabilized with yttrium oxide (Y-PSZ), Mg-PSZ is less subject to thermal degradation at temperatures below 200 °C [14,16]. For simplicity, the used material will from here on be referred to as ZrO_2. Its main fields of application include dental and medical engineering as well as high-temperature environments, such as gas turbines and industrial furnaces [15–21]. The workpiece material is furthermore characterized by an average size of crystallites of d_c = 50 μm, a density of ρ_w = 5.7 kg/dm^3, a toughness of K_{Ic} = 6.3 MPa·m$^{0.5}$, and a Young's modulus of E_w = 185 GPa. The workpieces themselves were of the dimensions 200 × 200 × 20 mm^3 and were plane-ground by the manufacturer, Figure 2, yielding an average arithmetic mean roughness of Ra = 1.0 μm.

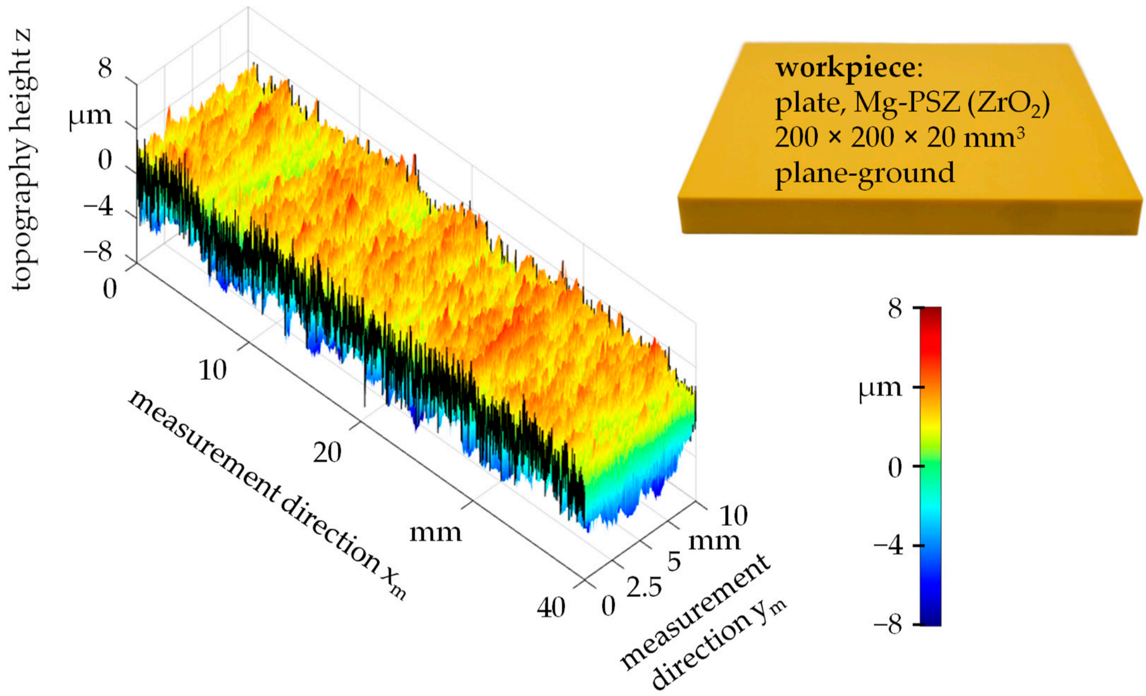

Figure 2. Topography of the plane-ground workpieces prior to brushing.

The abrasive brushing tools used were round brushes manufactured by CARL HILZINGER-THUM GMBH AND CO. KG, Tuttlingen, Germany, with a tool width of b_b = 20 mm and outer diameters between d_b = 340 mm and d_b = 380 mm. Tools with large diameters were chosen based on their large number of filaments N_f and the improved support between filaments due to their lower brush body curvature, thereby leading to more efficient brushing processes. The high hardness and the brittle machining behavior of ZrO_2 necessitate the use of polycrystalline diamond as an abrasive medium, bonded in a filamentary PA 6.12 matrix, a polyamide type with high restoration capability after liquid absorption. In order to investigate the relations between high material removal and low resulting surface roughness, three different grain sizes d_g and filament diameters d_f were used, Table 1. In addition, three different filament lengths l_f were investigated, Table 1, based on the correlation between increasing filament lengths l_f and decreasing process normal forces F_n [5].

Table 1. Brushing tool specification parameters.

Grain Size d_g	Filament Diameter d_f	Filament Length l_f
mesh (µm)	mm	mm
320 (29.2)	0.6	30
240 (44.5) *	1.0 *	40 *
80 (185)	1.4	50

* Default value.

The technological investigations were carried out on a gear profile grinding machine of type ZP 12 by KAPP NILES GMBH & CO. KG, Coburg, Germany, Figure 3a, and modified for plane brushing with a purpose-built setup, Figure 3b. Although the thermal conductivity of the workpiece material was specified as 3.0 W/(m·K) at room temperature, which is low compared to previously investigated metals, no cooling lubricant was used during brushing. This choice was made in order to decrease the number of possible influences on the measurement of process forces and the work result, as the polyamide matrix of the abrasive filaments is prone to the absorption of liquids, which increases their elasticity and in turn decreases the process forces [3,4].

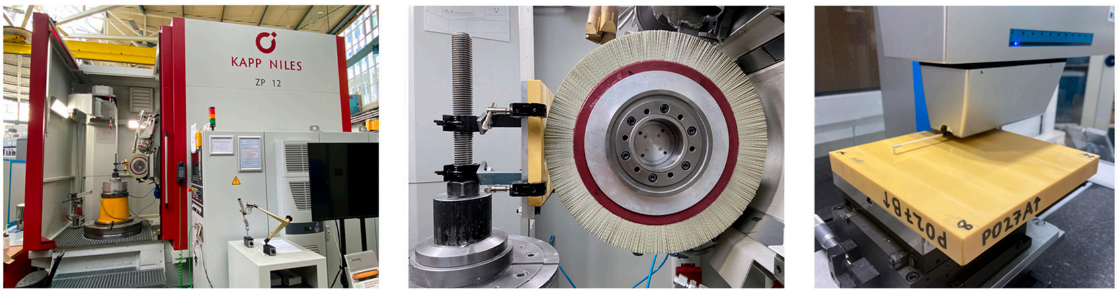

(**a**) (**b**) (**c**)

Figure 3. Experimental setup: (**a**) Brushing machine ZP 12; (**b**) experimental setup with ZrO_2 workpiece and round brush; (**c**) tactile surface measurement with Nanoscan 855.

The essential process parameters are the brushing velocity v_b, the tangential feed rate v_{ft}, and the infeed a_e [1–5], and the experiments were carried out as a fractional factorial design with three stages per parameter, Table 2. For consistency, all workpieces were brushed only once and in counter rotation, meaning that the brushing velocity v_b and the tangential feed rate v_{ft} pointed in opposite directions; however, the influence of the feed direction is estimated to be negligible due to the brushing velocity v_b being approximately three orders of magnitude higher than the tangential feed rate v_{ft}. Prior to the technological investigations, all brushing tools were worn in for 200 brushing cycles using default parameters; this was to maximize the consistency of the work result, as newly manufactured brushing tools tend to achieve higher material removal rates Q_w than worn-in brushing tools, the material removal rates Q_w of which are rapidly decreasing as tool wear sets in.

Table 2. Process parameter variation.

Brushing Velocity v_b	Tangential Feed Rate v_{ft}	Infeed a_e
m/s	**mm/min**	**mm**
10	200 *	1 *
20 *	500	2
30	1000	3

* Default value in fractional factorial design.

The correlation between process parameters and process forces dictates that a high brushing velocity v_b strongly increases the normal force F_n due to the large number of filament–workpiece contacts. In contrast, a large infeed a_e increases the normal force F_n distinctly less, whereas the tangential feed rate v_{ft} does not distinctly influence the normal force F_n [5,8,9]. Typically, the normal force F_n is represented by a static mean value $F_{n,\mu}$ over a time span of relative constancy, Figure 4a. Since brushing processes may be subject to dynamic filament behavior [8,9,22], the normal force F_n should furthermore be specified by the dynamic normal force $F_{n,\sigma}$, representing the standard deviation of the normal force F_n over the same time span of relative constancy.

Prior and subsequent to brushing, the surface roughness of each workpiece was measured with a tactile surface measurement device of type Nanoscan 855 by Hommel-Etamic GmbH, Villingen-Schwenningen, Germany, Figure 3c. As the surface roughness is inhomogeneous across the width of a brushed profile [5], it was always measured starting at the profile center to achieve high repeatability. Each experiment and each roughness measurement were repeated three times, yielding nine measurements per process parameter combination. For selected parameter combinations, topography measurements across the entire width of the brushed profile were carried out in order to determine the profile width w_b and the profile depth h_b, Figure 4b.

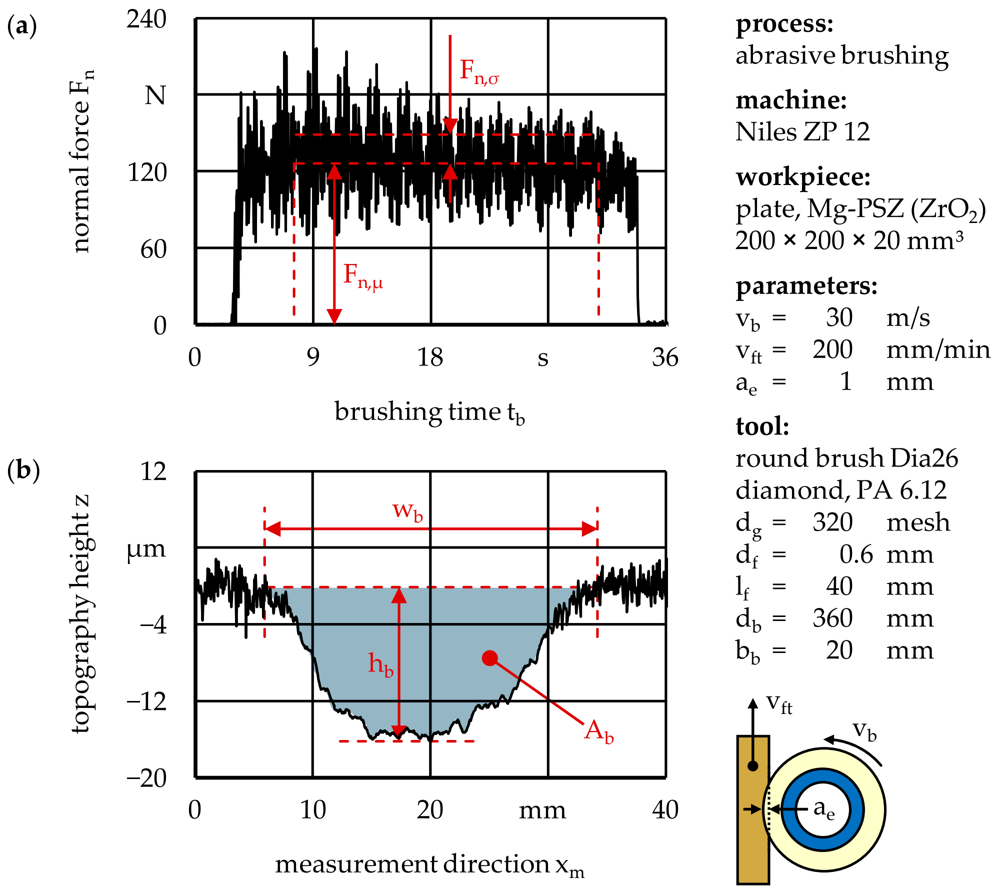

Figure 4. Determination of experimental parameters: (**a**) Static normal force $F_{n,\mu}$ and dynamic normal force $F_{n,\sigma}$; (**b**) profile width w_b, profile depth h_b, and profile cross-section area A_b.

By measurement of the height of the profile z, consisting of discrete data points z_i, and subsequent determination of the profile width w_b, the profile cross-section area A_b and the material removal rate Q_w can be calculated:

$$A_b = \int_{w_b} z \cdot dx_m \quad (1)$$

$$Q_w = A_b \cdot v_{ft} \quad (2)$$

As the profile depth h_b may be far greater than the surface roughness, depending on the tool specification and the process parameters, it indicates whether only the roughness peaks are removed as intended or an entirely new topography is formed by the brushing process, similar to a grinding process. Hence, the profile depth h_b serves as a measure for the workpiece geometry deviation, which is treated as undesirable within the scope of this article.

3. Results

The brushing velocity v_b being the most influential process parameter, it was confirmed to have a distinct impact on the normal force F_n exerted by the brushing tool onto the workpiece, which means that increasing brushing velocities v_b always leads to ascending normal forces F_n, Figure 5.

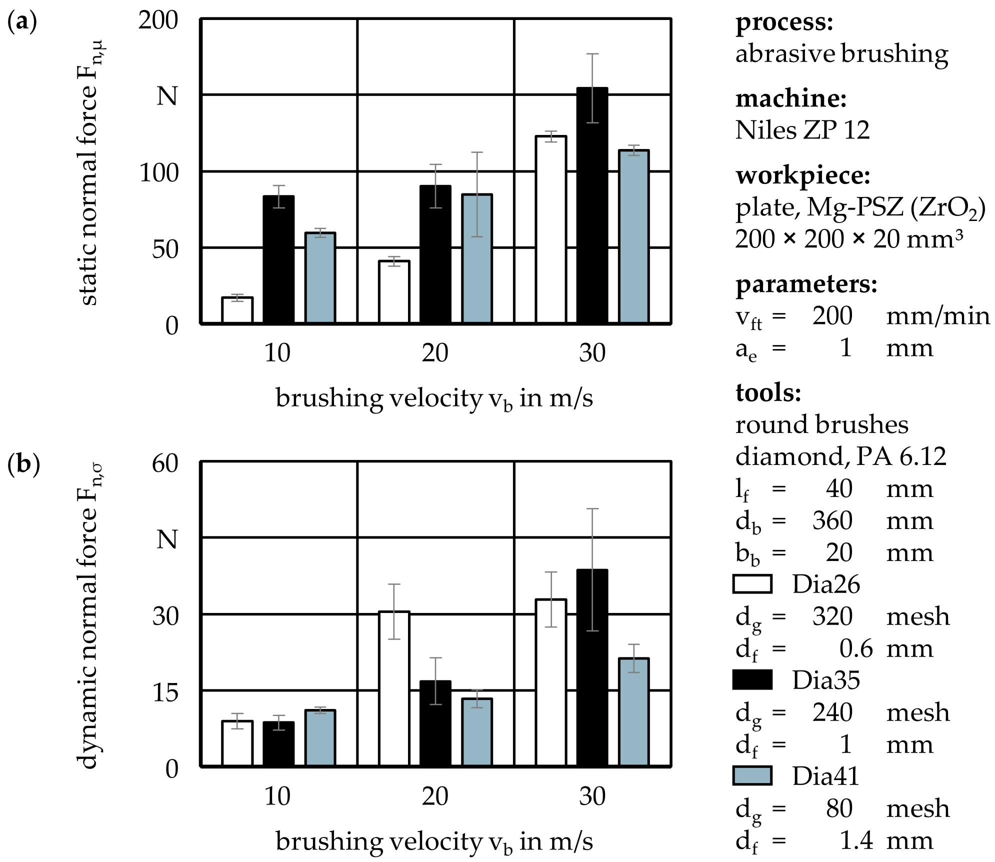

Figure 5. Dependence of the normal force F_n on the brushing velocity v_b under variation of grain size d_g and filament diameter d_f: (**a**) Static normal force $F_{n,\mu}$; (**b**) dynamic normal force $F_{n,\sigma}$.

A notable result of analyzing the static normal force $F_{n,\mu}$ is that the highest values were not achieved by tool Dia41 with the largest filament diameter d_f = 1.4 mm, but instead by Dia35 with a filament diameter of only d_f = 1.0 mm, Figure 5a, despite filaments of large diameters d_f being stiffer, theoretically leading to larger contact forces. This can be explained by the total number of filaments N_f counteracting the stiffness of the single filament: Whereas tool Dia41 has an approximate filament number of N_f = 7850, Dia35 consists of approximately N_f = 10,900 filaments, which are closer together due to their smaller filament diameter d_f, and thus, better supported due to a higher stocking density. This is assumed to also cause the progressive increase in the static normal force $F_{n,\mu}$ for tool Dia26 with the smallest filament diameter of d_f = 0.6 mm and an approximate filament number of N_f = 37,900, the total number of filament–workpiece contacts per time influencing the normal force F_n more than the individual filament stiffness.

Analysis of the dynamic normal force $F_{n,\sigma}$ suggests dynamic tool behavior for Dia26 at brushing velocity v_b = 20 m/s, indicated by a strongly degressive trend as opposed to tools Dia35 and Dia41, Figure 5b. High dynamic normal forces $F_{n,\sigma}$ caused by dynamic tool behavior are assumed to have no positive influence on the work result, despite overall larger normal forces F_n, but are on the contrary associated with increased tool wear due to high filament stress [22].

Indeed, analysis of the work result shows that at brushing velocity v_b = 20 m/s, tool Dia26 neither reduced the workpiece roughness considerably nor removed a notable amount of workpiece material, Figure 6. Instead, highest roughness reduction with tool Dia26 was achieved by a high brushing velocity of v_b = 30 m/s, resulting in a reduction in the arithmetic mean roughness of ΔRa = 85%, Figure 6a, superseding all other experiments. Additionally, small grain sizes d_g and filament diameters d_f lead to a progressive trend, meaning a more efficient roughness reduction at high brushing velocities v_b. Contrary to this, tools with large grain sizes d_g and filament diameters d_f yield average surface roughness reductions, which are largely independent of the brushing velocity v_b due to the grain size d_g being the limiting factor of the low-threshold roughness.

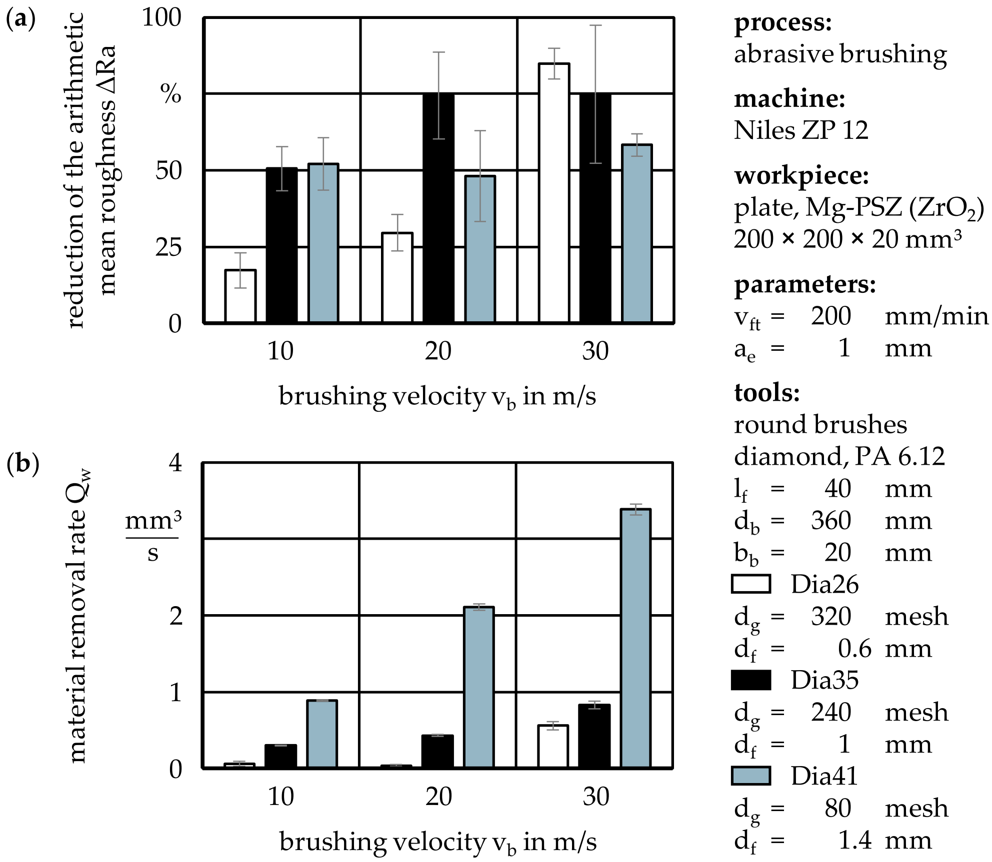

Figure 6. Dependence of the work result on the brushing velocity v_b under variation of grain size d_g and filament diameter d_f: (**a**) Reduction in the arithmetic mean roughness ΔRa; (**b**) material removal rate Q_W.

Further noticeable is the strong deviation between experiments regarding the dynamic normal force $F_{n,\sigma}$ and the reduction in the arithmetic mean roughness ΔRa for tool Dia35 and brushing velocity v_b = 30 m/s, suggesting a correlation between both as well as a negative influence of dynamic tool behavior.

In terms of the material removal rate Q_W, large grain sizes d_g and filament diameters d_f are more efficient at high brushing velocities v_b, Figure 6b, exhibiting an almost proportional trend. By contrast, small grain sizes d_g and filament diameters d_f lead to a progressive trend, qualitatively resembling the static normal force $F_{n,\mu}$, Figure 5a. However, if low geometrical deviations are required, high material removal rates Q_W are undesirable, as they compulsorily lead to large profile depths h_b.

As the arithmetic mean roughness Ra may not be meaningful for all applications, an in-depth look is taken at two roughness parameters characterizing the tribological properties of a surface: the reduced peak height Rpk, resembling the tribologically disadvantageous peaks of a roughness profile, and the reduced valley depth Rvk, resembling the tribologically advantageous valleys, in which microscopic volumes of lubricant are retained. Concerning the reduction in the reduced peak height ΔRpk, Figure 7a, both tool specifications Dia35 with medium and Dia41 with large grain size d_g and filament diameter d_f appear to remove roughness peaks regardless of the brushing velocity v_b, the remaining peaks being newly formed and their height depending only on the grain size d_g, whereas tool Dia26 with small grain size d_g and filament diameter d_f is suited for deliberate peak height adjustment. Large standard deviations between experiments suggest an unreliable brushing process and further confirm that new peaks of varying height were formed.

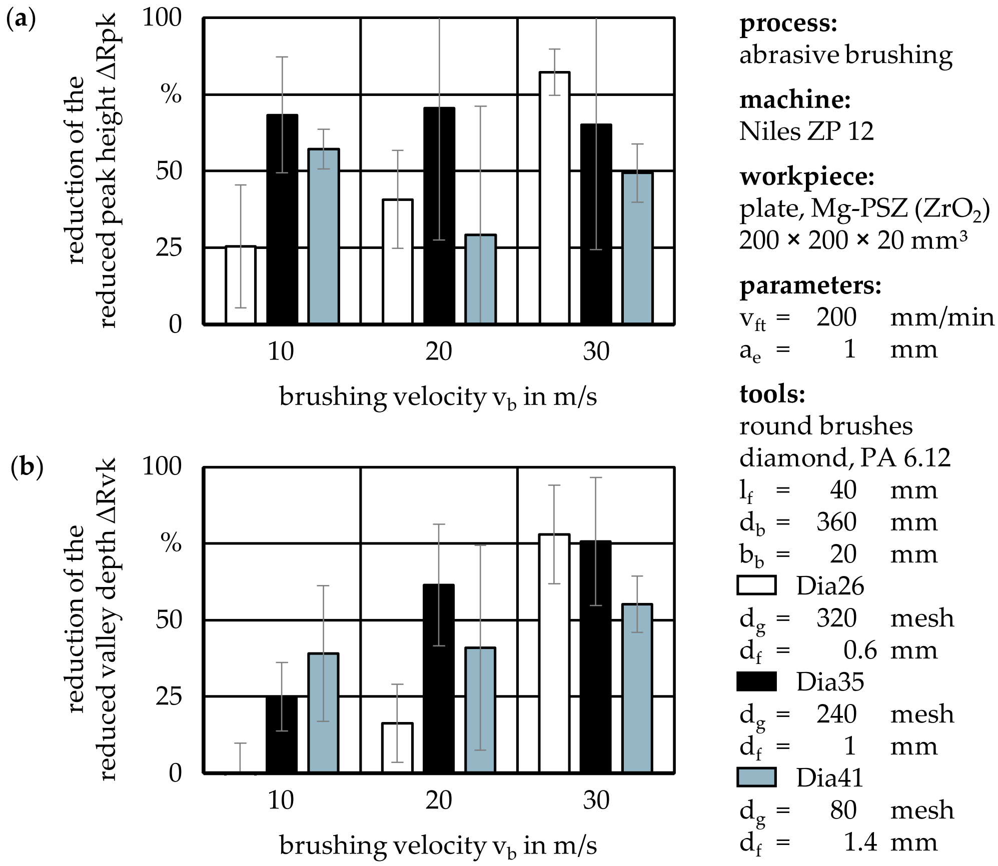

Figure 7. Dependence of the tribological roughness profile characterization on the brushing velocity v_b under variation of grain size d_g and filament diameter d_f: (**a**) Reduction in the reduced peak height ΔRpk; (**b**) reduction in the reduced valley depth ΔRvk.

Analogously, the reduction in the reduced valley depth ΔRvk shows a similar, albeit amplified trend, Figure 7b, tool Dia35 with medium grain size d_g and filament diameter d_f seeming suitable for deliberate valley depth adjustments by variation of the brushing velocity v_b. Dia26 with small grain size d_g and filament diameter d_f exhibits this adjustability even more, at brushing velocity v_b = 10 m/s removing none of the roughness valleys induced by the initial plane-grinding treatment and at brushing velocity v_b = 30 m/s removing nearly all.

Figure 8 shows the workpiece topography after one-time brushing with grain size d_g = 240 mesh, filament diameter d_f = 1 mm, and brushing velocity v_b = 10 m/s. The roughness peaks were mostly removed, denoted by a reduction in the reduced peak height of ΔRpk = 68%, while the roughness valleys remain largely intact, denoted by a reduction in the reduced valley depth of ΔRvk = 25%. This corresponds to a reduction in the arithmetic mean roughness ΔRa = 51% and a profile depth of h_b = 4.120 µm, meaning little shape deviation considering the initial total height of the roughness profile Rt = 8.403 µm.

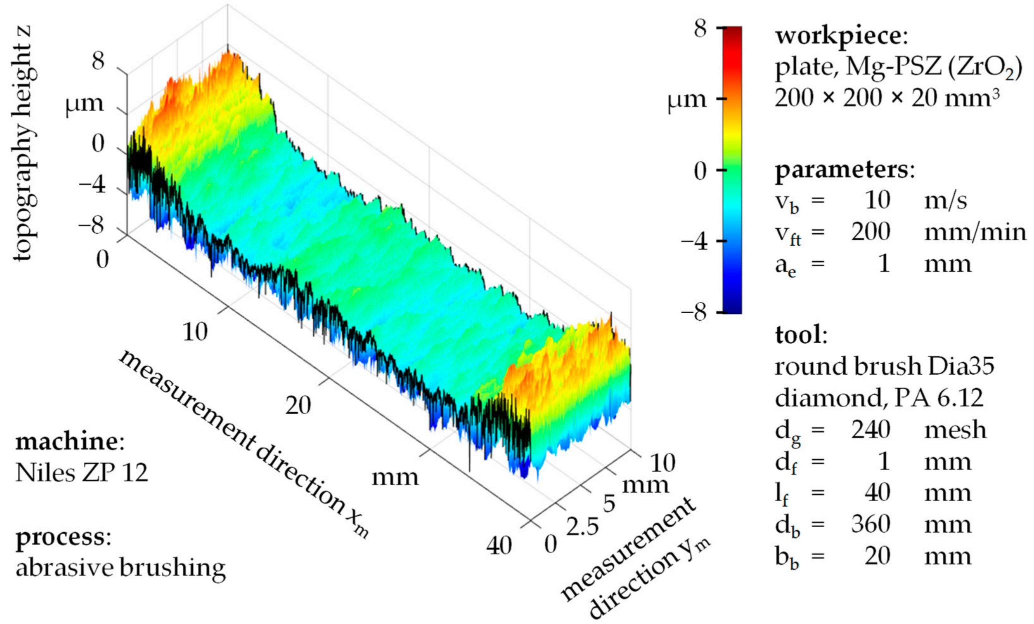

Figure 8. Topography of ZrO_2 workpiece after brushing with grain size d_g = 240 mesh, filament diameter d_f = 1 mm, and brushing velocity v_b = 10 m/s.

In comparison, Figure 9 shows a similar process with increased brushing velocity v_b = 30 m/s. Not only were roughness peaks and valleys mutually removed, denoted by reductions in the reduced peak height of ΔRpk = 65% and the reduced valley depth of ΔRvk = 76%, but also was a considerable shape deviation induced, denoted by a profile depth of h_b = 13.558 µm.

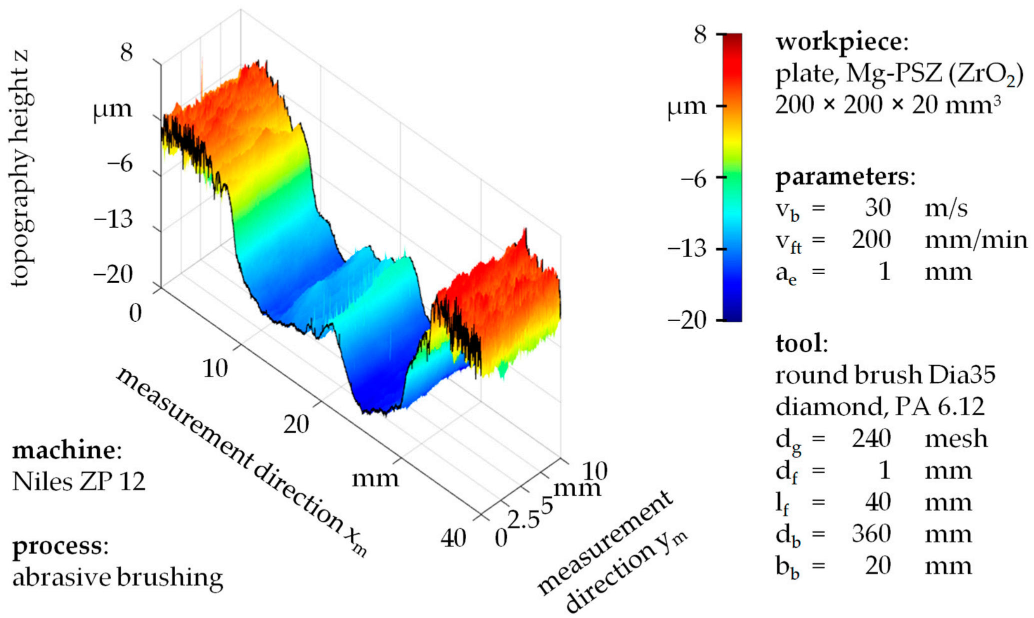

Figure 9. Topography of ZrO_2 workpiece after brushing with grain size d_g = 240 mesh, filament diameter d_f = 1 mm, and brushing velocity v_b = 30 m/s.

The process also shows the characteristic W-shape observed in previous studies [5,7], caused by the abrasive filaments deflecting to the sides according to the principle of least constraint, although previously no remark was made on the asymmetry of the W-shape. By contrast, Figure 10 depicts the topography of an analogous process with grain size

d_g = 320 mesh and filament diameter d_f = 0.6 mm, which shows a U-shaped profile instead of a W-shape despite a comparable profile depth of h_b = 10.036 µm.

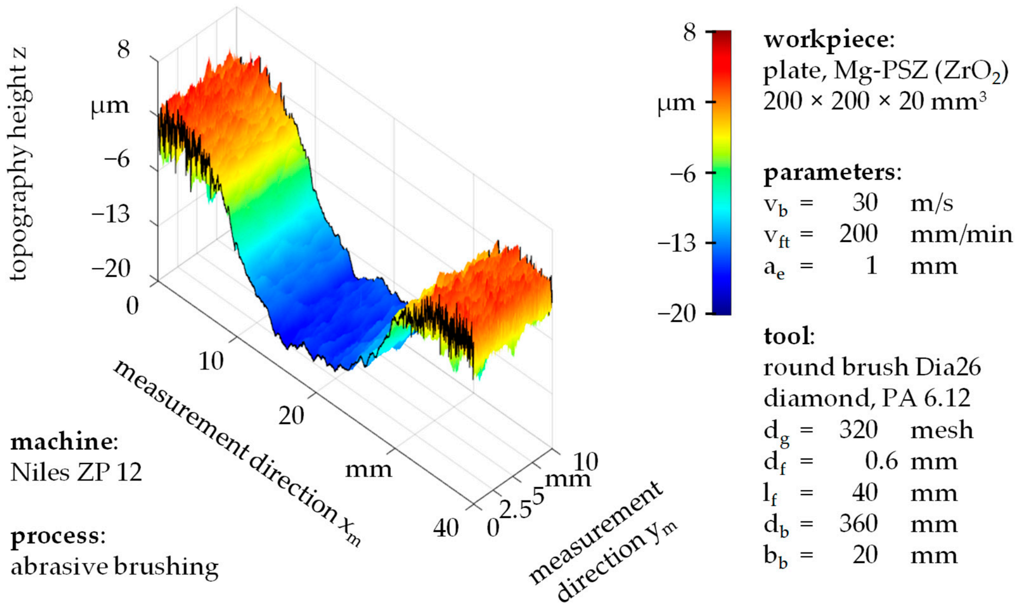

Figure 10. Topography of ZrO_2 workpiece after brushing with grain size d_g = 320 mesh, filament diameter d_f = 0.6 mm, and brushing velocity v_b = 30 m/s.

Figure 11 shows an exemplary process of extreme shape deviation, induced by grain size d_g = 80 mesh, filament diameter d_f = 1.4 mm, and brushing velocity v_b = 20 m/s. The initial roughness peaks and valleys were altogether removed, instead inducing new macroscopic peaks and valleys at a profile depth of h_b = 38.483 µm, which exceed the initial total height of the roughness profile of Rt = 9.171 µm.

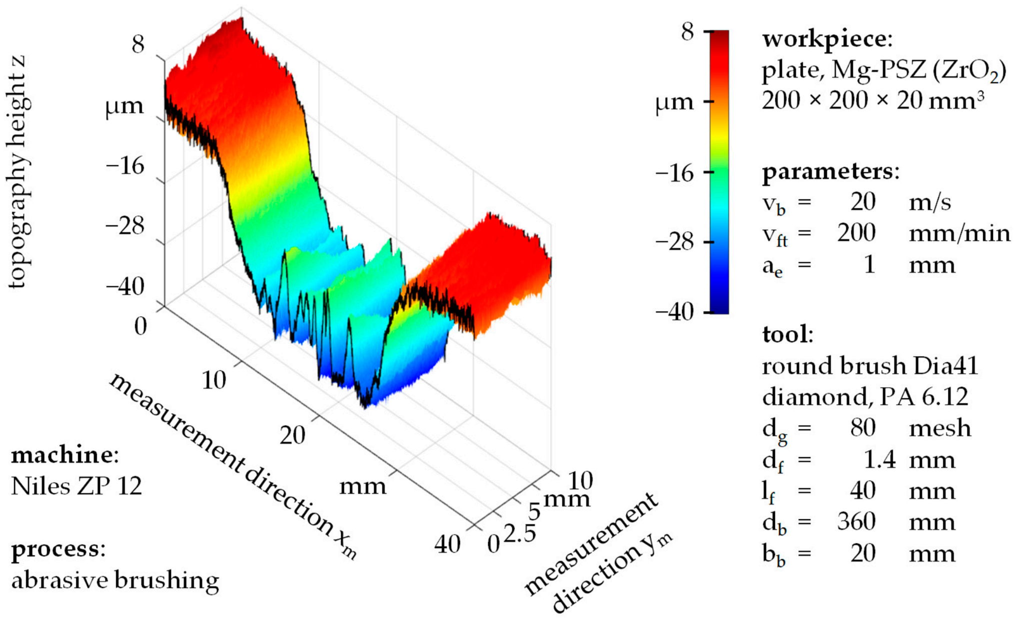

Figure 11. Topography of ZrO_2 workpiece after brushing with grain size d_g = 80 mesh, filament diameter d_f = 1.4 mm, and brushing velocity v_b = 20 m/s.

Moving on to the next relevant process parameter, the tangential feed rate v_{ft}, previous studies agree on a proportional response of the work result, meaning that one-time brushing at a decreased tangential feed rate v_{ft} has the same effect as multiple brushing cycles at a high tangential feed rate v_{ft}, given that both processes overall amount to the same brushing time [4,5,7]. This is mostly contributed to the tangential feed rate v_{ft} being approximately three orders of magnitude lower than the brushing velocity v_b, leading to the tangential feed rate v_{ft} being omitted as a relevant parameter from several studies with a focus on the process forces due to its theoretical proportionality to the work result [8,9,22]. Indeed, the technological investigations carried out within the scope of this article confirmed an independence of the process forces from the tangential feed rate v_{ft}. Nonetheless, for practical purposes multiple brushing cycles at a high tangential feed rate v_{ft} may be advisable while dry-brushing ceramics due to their low thermal conductivity, spreading the induced process heat across a larger surface, thus reducing tool wear.

Comparing the reduction in the arithmetic mean roughness ΔRa for different tangential feed rates v_{ft}, grain sizes d_g, and filament diameters d_f, as shown in Figure 12a, it becomes apparent that comparably large roughness reduction is achieved at a tangential feed rate of v_{ft} = 1000 mm/min, whereas lower tangential feed rates v_{ft} do not reduce the arithmetic mean roughness Ra proportionally more, meaning that high tangential feed rates v_{ft} lead to more efficient brushing processes. More importantly, this applies to all investigated tool specifications, the grain size d_g being the limiting factor in achieving high roughness reduction.

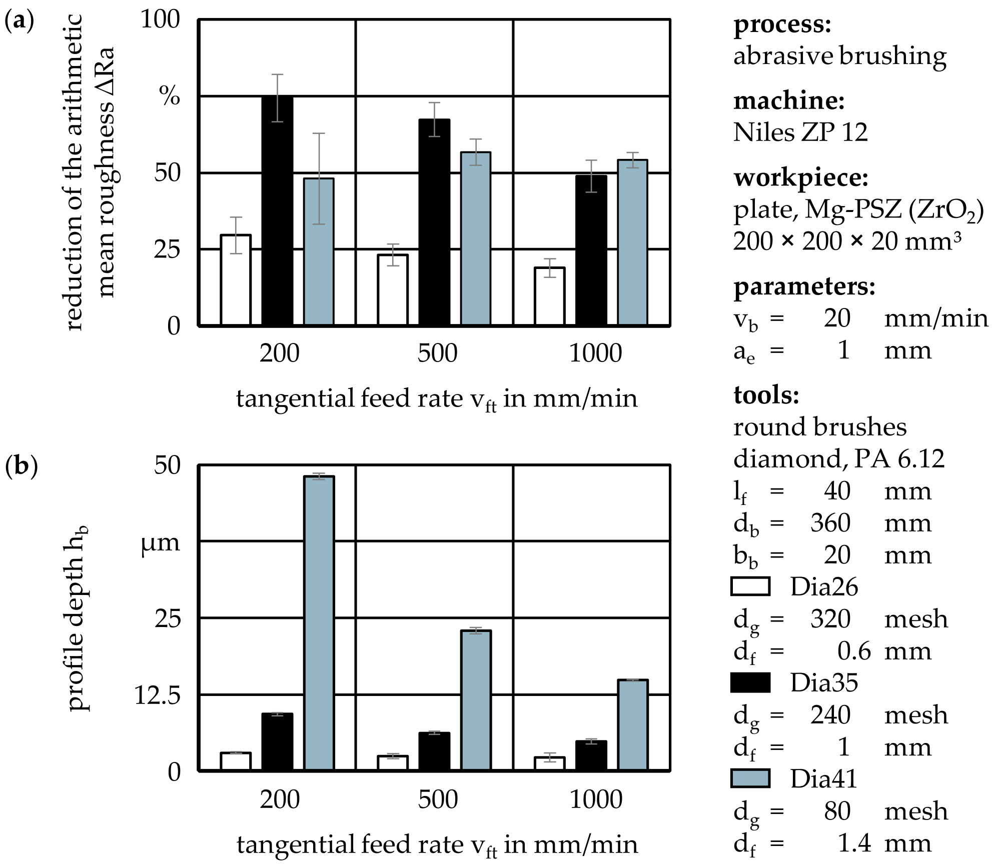

Figure 12. Dependence of the work result on the tangential feed rate v_{ft} under variation of grain size d_g and filament diameter d_f: (**a**) Reduction in the arithmetic mean roughness ΔRa; (**b**) profile depth h_b.

In comparison, the profile depth h_b shows similar behavior, Figure 12b, that is for small grain sizes d_g and filament diameters d_f, while tool Dia41 with grain size d_g = 80 mesh and filament diameter d_f = 1.4 mm shows a behavior more proportional to the tangential feed rate v_{ft}, meaning that it is a suitable parameter to adjust undesirable shape deviations. As the reduction in the arithmetic mean roughness Ra seems to be independent of the tangential feed rate v_{ft} using tool Dia41, it stands to reason to increase the tangential feed rate v_{ft} beyond the investigated parameter space to achieve even lower shape deviations and comparably high roughness reductions.

Figure 13 shows a topography of a workpiece brushed with grain size d_g = 240 mesh, filament diameter d_f = 1 mm, and tangential feed rate v_{ft} = 1000 mm/min. Despite the small profile depth of h_b = 3.837 µm, a W-shape is setting in, distinguished by the obvious crest in the tool center region, marking a region of little surface treatment. The topography is characterized by reductions in the arithmetic mean roughness of ΔRa = 49%, the reduced peak height of ΔRpk = 67%, and the reduced valley depth of ΔRvk = 23%, resembling the largest difference between roughness peak height and valley depth among all experiments conducted within the scope of this article.

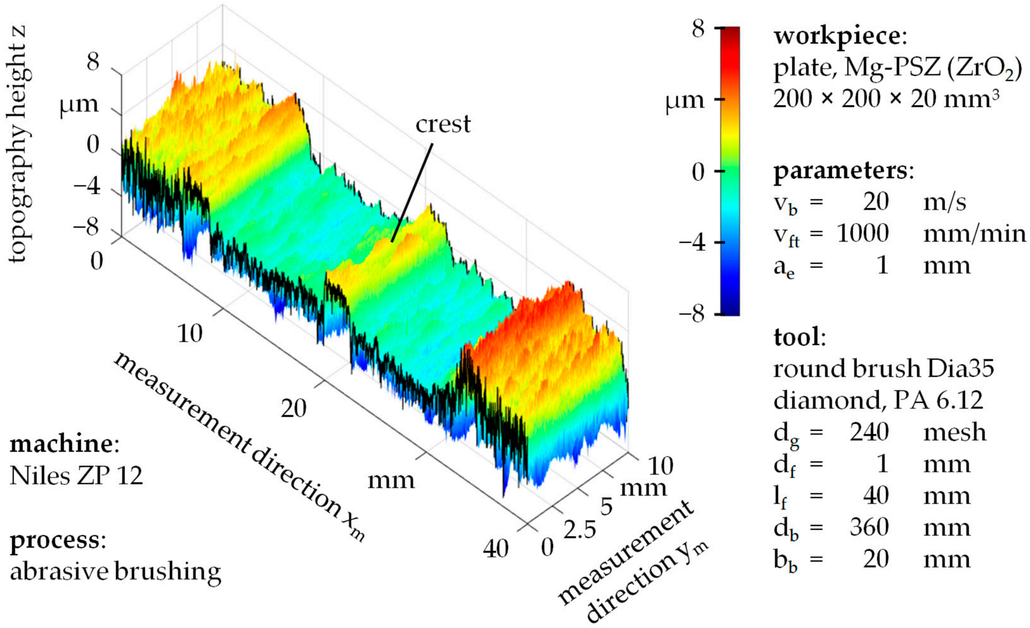

Figure 13. Topography of ZrO_2 workpiece after brushing with grain size d_g = 240 mesh, filament diameter d_f = 1 mm, and tangential feed rate v_b = 1000 mm/min.

Approaching the third and final relevant process parameter, the infeed a_e showed distinguishable effects on the work result under variation of the filament length l_f. Unfortunately, not all tool specifications proved suitable for the chosen parameter space, as all tools with filament length l_f = 30 mm were permanently damaged even at low infeed a_e = 1 mm and moderate brushing velocity v_b = 20 m/s, Figure 14, mostly as a result of dry-brushing and the low thermal conductivity of ceramics. Consequently, only tools with filament lengths l_f = 40 mm and l_f = 50 mm could be properly investigated.

Figure 14. Brushing tool Dia28 permanently damaged by process heat, caused by a disadvantageous combination of filament length l_f = 30 mm and the process parameters.

Analyzing the process forces under variation of infeed a_e and filament length l_f, Figure 15a, shows two expected trends: large infeeds a_e and small filament lengths l_f each leading to increased static normal forces $F_{n,\mu}$, one being a result of increased filament stress, the other of increased filament stiffness, which confirms the findings of all previous studies [3–5,7–9,22]. However, not as trivial is the finding that the dynamic normal force $F_{n,\sigma}$, which has not yet been thoroughly investigated, shows an opposite trend, meaning that large infeeds a_e and small filament lengths l_f each lead to decreased dynamic normal forces $F_{n,\sigma}$, Figure 15b. Moreover, brushing processes with filament length l_f = 50 mm exhibit larger deviations between experiments, further corroborating dynamic tool behavior.

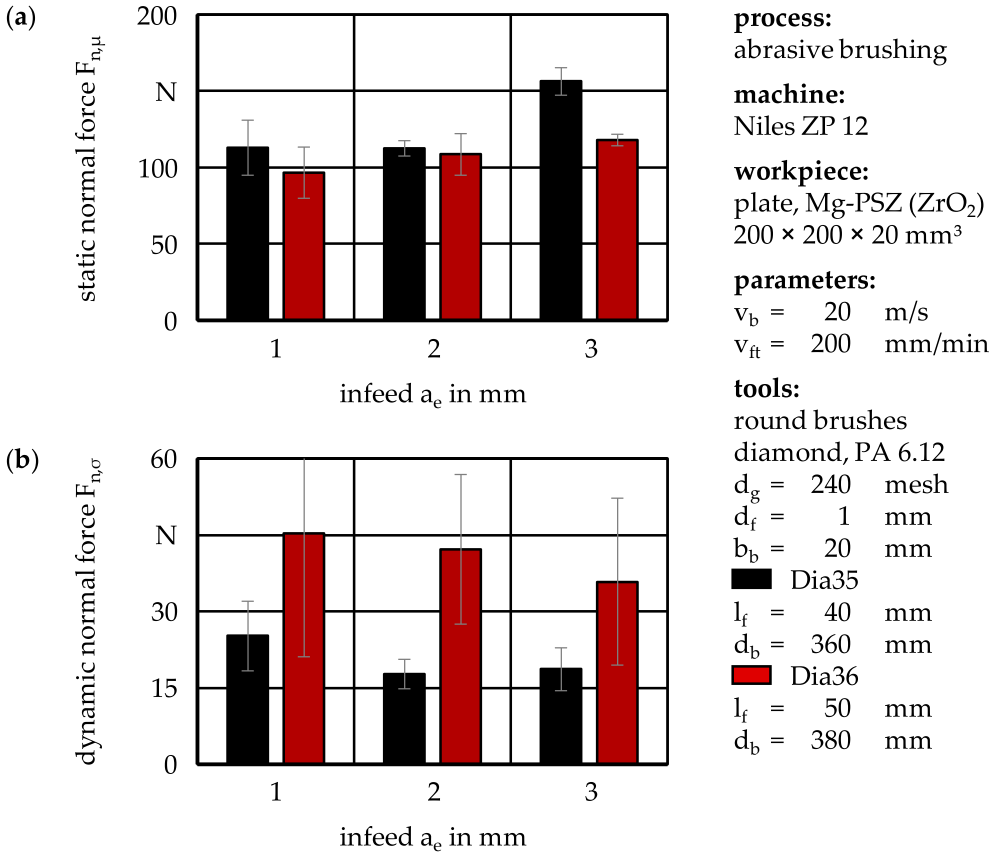

Figure 15. Dependence of the normal force F_n on the infeed a_e under variation of grain size d_g and filament diameter d_f: (**a**) Static normal force $F_{n,\mu}$; (**b**) dynamic normal force $F_{n,\sigma}$.

This decrease in the dynamic normal force $F_{n,\sigma}$ with increased infeed a_e is likely a result of prolonged filament–workpiece contact, resulting in both an increased contact time t_c and a larger contact length l_c, leading to a larger number of abrasive filament beings in contact with the workpiece simultaneously, thus stabilizing the process.

Contrasting these findings with the reduction in the arithmetic mean roughness Ra, Figure 16a, opposing behaviors for the two investigated tool specifications can be observed: while tool Dia35 with filament length l_f = 40 mm shows maximum roughness reduction at an infeed of a_e = 2 mm, exhibiting a discontinuous trend, tool Dia36 with filament length l_f = 50 mm achieved highest roughness reduction at maximum infeed a_e = 3 mm, furthermore represented by a low deviation between experiments, accounting for an exceptionally stable and repeatable brushing process.

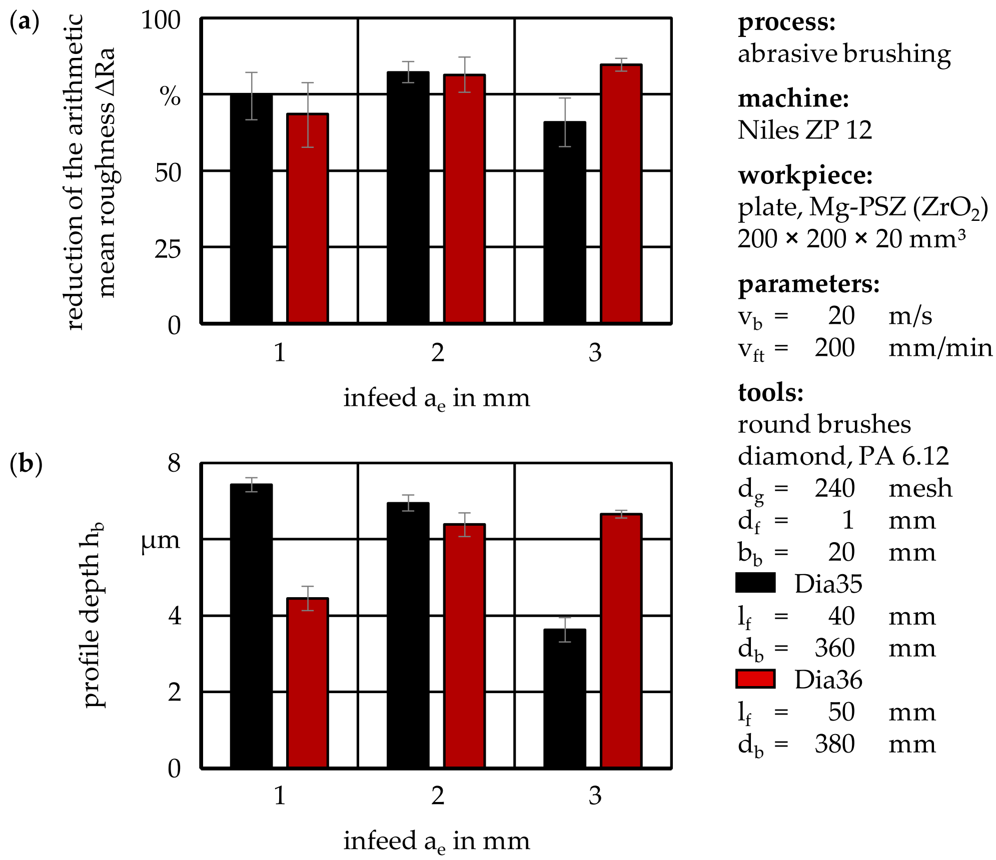

Figure 16. Dependence of the work result on the infeed a_e under variation of grain size d_g and filament diameter d_f: (**a**) Reduction in the arithmetic mean roughness ΔRa; (**b**) profile depth h_b.

These trends appear reinforced when compared with the profile depth h_b, Figure 16b, which at increased infeed a_e decreases progressively for filament length l_f = 40 mm and increases degressively for filament length l_f = 50 mm, meaning in fact that brushing processes with small filament lengths l_f lead to less shape deviation at high infeeds a_e, whereas large filament lengths l_f cause less shape deviation at low infeeds a_e. However, the overall values of the profile depth h_b remain below the initial total heights of the roughness profile, ranging from Rt = 7.485 µm to Rt = 8.399 µm, which makes brushing processes with large filament lengths l_f and infeeds a_e very suitable for the deliberate adjustment of the surface roughness, while simultaneously inducing only small shape deviations. Nonetheless, the exact interrelations between filament length l_f, infeed a_e, and work result remain inconclusive due to the opposing behaviors of tools Dia35 and Dia36, requiring more technological investigations while dividing the parameter space into finer increments.

Figure 17 shows the workpiece topography of a brushing process with filament length l_f = 50 mm and infeed a_e = 3 mm, characterized by reductions in the arithmetic mean roughness of ΔRa = 85%, the reduced peak height of ΔRpk = 83%, and the reduced valley depth of ΔRvk = 76%, albeit a relatively small profile depth h_b = 6.653 µm, making it the most efficient brushing process in terms of high roughness reduction and low shape deviation among all conducted experiments. Also notable is the asymmetry of the forming W-shape, similar to Figure 9; this might be contributed to either an incorrect orientation of the workpiece relative to the brushing tool or the manufacturing process of the brushing tool itself.

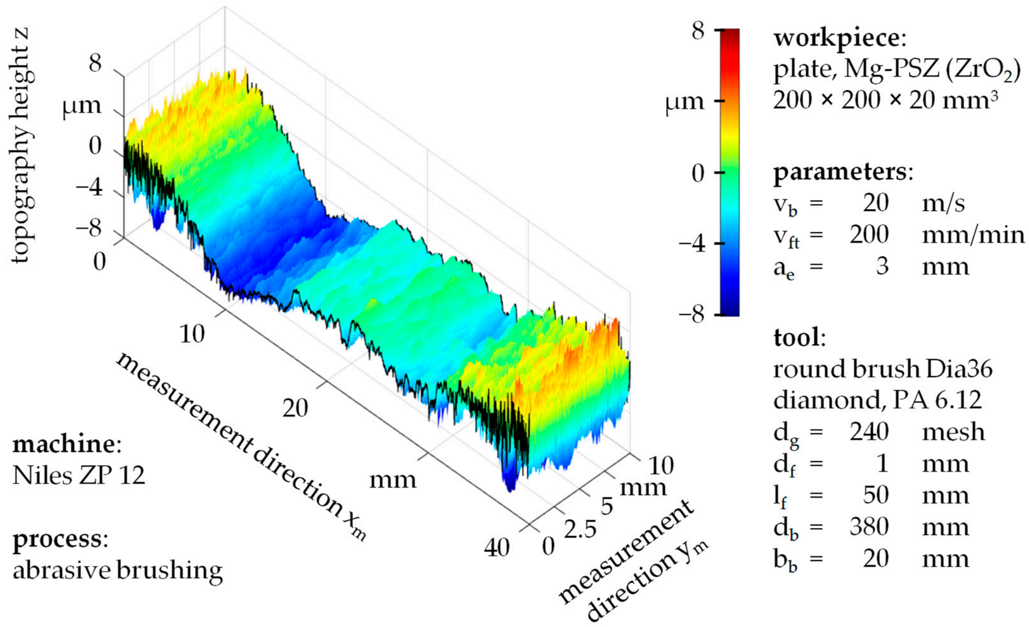

Figure 17. Topography of ZrO_2 workpiece after brushing with grain size d_g = 240 mesh, filament diameter d_f = 1 mm, filament length l_f = 50 mm, and infeed a_e = 3 mm.

On a side note, it should be mentioned that brushing with an infeed of $a_e < 1$ mm is theoretically possible, but potentially ineffective due to the eccentricity of the brushing tools: depending on the measurement position, the actual tool diameter $d_{b,a}$ deviates up to ± 0.5 mm from the nominal tool diameter of d_b = 380 mm; this is purely a result of the tool manufacturing process, specifically the filament tips being sheared off to their nominal length as a final manufacturing step. Therefore, not the entirety of abrasive filaments would be in contact with the workpiece if an infeed of $a_e < 1$ mm were chosen. To minimize this inevitable diameter deviation, brushing tools may be dressed with an abrasive workpiece or a dressing stone prior to usage. However, as part of these technological investigations, it was found that such dressing processes were highly inefficient due to the abrasive nature of bonded polycrystalline diamond, resulting in rapidly blunted dressing stones, the pores of which are clogged with polymer residue, and the polymer matrix of the filament tips becoming frayed rather than cylindrical. Hence, the industrial fine-dressing of relatively inexpensive abrasive brushing tools would be too costly in the current state of technology.

4. Discussion and Conclusions

Within the scope of this article, technological investigations with abrasive brushing tools on plane-ground ZrO_2 workpieces were conducted, factorially varying the tool specification parameters grain size d_g, filament diameter d_f, and filament length l_f, as well as the process parameters brushing velocity v_b, tangential feed rate v_{ft}, and infeed a_e. All processes were carried out without the use of cooling lubricant and as single brushing cycles.

During the evaluation of the work result, focus was laid on minimal workpiece geometry deviation, denoted by the profile depth h_b, and the reduction in the surface roughness, either in the form of the arithmetic mean roughness Ra or the more nuanced parameters reduced peak height Rpk and reduced valley depth Rvk, locating the transition between the mere removal of the roughness peaks and the total removal of the initial roughness profile, as both cases may be of use depending on whether an application requires the material to be lubricated or not.

Based on the presented work, the following conclusions can be drawn:

- High contact forces are not necessarily achieved by stiff abrasive filaments of large filament diameters d_f, but instead by high filament stocking densities typical for small

filament diameters d_f. This effect is amplified with increased brushing velocity v_b due to the larger number of filament–workpiece contacts per time.
- Due to the higher stocking density, small filament diameters d_f also lead to more homogeneous brushing profiles, characterized by U-shapes as opposed to W-shapes, because increased support between filaments prevents them from deflecting to the sides.
- Brushing tools with small grain sizes d_g and filament diameters d_f decrease the surface roughness more effectively at high brushing velocities v_b. In contrast, tools with large grain sizes d_g and filament diameters d_f decrease the surface roughness effectively at low brushing velocities v_b, the grain size d_g being the limiting factor, and high brushing velocities v_b only increasing undesirable shape deviations.
- The smaller grain size d_g and filament diameter d_f are, the wider becomes the range of different brushing velocities v_b to control the transition between mere reduction in the roughness peaks and total removal of the initial roughness profile. Alternatively, high tangential feed rates v_{ft} can be used at the cost of homogeneity of the brushed profile.
- ZrO_2 should be brushed at high tangential feed rates v_{ft} in order to reduce thermal damage to the tools and shape deviation to the workpieces, as material removal happens more rapidly than in comparable brushing processes on metallic workpieces. For the same reasons, the use of tools with short filament lengths l_f is advised against.
- High reduction in the surface roughness, small shape deviations, and stable work results can be achieved with large filament lengths l_f and infeeds a_e. However, tools with small filament lengths l_f tendentially perform less effectively at large infeeds a_e.

In respect of these conclusions, several recommendations can be made regarding abrasive brushing of ceramics with bonded diamond grains, laying focus on maximum roughness reduction and minimum shape deviation: the authors recommend process designs with grain sizes of $d_g \geq 240$ mesh, filament diameters of $d_f \leq 1$ mm, filament lengths of $l_f \geq 40$ mm, preferably large tool diameters d_b, and tangential feed rates of $v_{ft} \geq 1000$ mm/min. For minimal and uniform tool wear, the infeed a_e should be chosen just large enough such that all filaments are equally in contact with the workpiece but axial filament deflection is kept to a minimum, especially with filament lengths of $l_f \leq 40$ mm. The brushing velocity v_b can then be increased successively to achieve the desired compromise between maximum roughness reduction and minimum shape deviation. If possible, oil-based cooling lubricant should be used during industrial brushing processes in order to compensate for low thermal conductivity and to remove the fine-grained wear products of ZrO_2, which are associated with minor health risks and could cause irritations of the respiratory tract if inhaled or ingested. Alternatively, wear products may be vacuumed off with a suitable ventilation system.

5. Outlook

Currently, the gathered data on tool specifications, process parameters, process forces, and work results are used to train a model, which provides prognoses on the brushing of ZrO_2. This can help with the design of brushing processes and tools, in particular when coupled with discrete element modeling, which would make it possible to apply knowledge gained on the brushing of planar workpieces to complexly shaped workpieces.

In addition, further technological investigations need to be carried out, specifically on the narrow application range of brushing tools with filament length $l_f = 30$ mm. High process forces indicate that these tools could be very effective for finishing ZrO_2 if used at low brushing velocities v_b, high tangential feed rates v_{ft}, and small infeeds a_e.

More technological investigations should also be carried out to distinguish between the influences of grain size d_g and filament diameter d_f, both of which were varied simultaneously within the scope of this article. In practice, this stands to reason because large grains are difficult to bond in thin polymer filaments with the goal of forming homogeneous abrasive filaments of constant Young's moduli. Vice versa, small grains bonded in thick filaments might prove ineffective because the majority of grains and cutting edges are encompassed by polymer and therefore not partaking in the finishing process. Nonetheless, as part of future investigations, both grain size d_g and filament diameter d_f should be treated as separate specification parameters in order to understand their individual influences. At this, the relationship between grain size d_g and the workpieces' microstructure and resistance to abrasive processing should be further examined.

So far, round brushes were used because the brushing velocity v_b pertains to the entirety of abrasive filaments and infeed a_e as well as brushing velocity v_b can be controlled as separate process parameters, whereas, for other tool shapes, the outer filaments move at higher brushing velocity v_b and the infeed a_e decreases with increasing brushing velocity v_b due to centrifugal forces deflecting the filaments outwards. However, round brushes are traditionally used for deburring, edge rounding, and gear flank finishing, not on plane surfaces. Therefore, other types of tool shapes should also be investigated for wider industrial applicability, for example, cup brushes, which are more common when finishing surfaces.

Author Contributions: Conceptualization, A.H. and E.U.; methodology, E.U.; software, A.H.; validation, A.H.; formal analysis, A.H.; investigation, A.H.; resources, A.H.; data curation, A.H.; writing—original draft preparation, A.H.; writing—review and editing, E.U.; visualization, A.H.; supervision, E.U.; project coordination, E.U.; funding acquisition, E.U. All authors have read and agreed to the published version of the manuscript.

Funding: This research was funded by the German Research Foundation (DFG) within the scope of the project "Analyse des Zerspan- und Verschleißverhaltens beim Bürstspanen mit abrasivem Medium sprödharter Werkstoffe" ("Analysis of the machining and wear characteristics during abrasive media brushing of brittle-hard materials"), project number 392312434. The authors kindly thank the funder for their support.

Institutional Review Board Statement: Not applicable.

Informed Consent Statement: Not applicable.

Data Availability Statement: Not applicable.

Conflicts of Interest: The authors declare no conflict of interest.

References

1. Uhlmann, E.; Lypovka, P.; Sommerfeld, C.; Bäcker, C.; Dethlefs, A.; Hochschild, L. Abrasives Bürsten. *Werkstatt Betr. (WB)* **2014**, *4*, 70–72.
2. Uhlmann, E.; Sommerfeld, C.; Renner, M.; Baumann, M. Bürstspanen von Profilen. *Werkstattstech. Online* **2017**, *107*, 238–243. [CrossRef]
3. Hochschild, L. Finishbearbeitung Technischer Oberflächen aus Gehärtetem Stahl unter Verwendung von Rundbürsten mit Schleiffilamenten. Ph.D. Thesis, Technical University Berlin, Berlin, Germany, 2018.
4. Uhlmann, E. Flexible Feinstbearbeitung von Funktionsflächen mit alternativen Werkzeugkonzepten (FlexFeinst). In *Schlussbericht zu IGF-Vorhaben Nr. 19601 N/1*; TIBKAT 1693827239; Technical University Berlin, Institute for Machine Tools and Factory Management: Berlin, Germany, 2020.
5. Sommerfeld, C. Modellbasierte Prozessvorhersagen für das Bürstspanen mit Gebundenem Schleifmittel. Ph.D. Thesis, Technical University Berlin, Berlin, Germany, 2022.
6. Rentschler, J.; Muckenfuß, G. Neue Anwendungsmöglichkeiten durch hochtemperaturbeständige Schleiffilamente in der Oberflächenbearbeitung. In *Jahrbuch Honen, Schleifen, Läppen und Polieren*; Hoffmeister, H.W., Denkena, B., Eds.; Vulkan: Essen, Germany, 2013; pp. 387–403.
7. Uhlmann, E.; Hoyer, A. Surface Finishing of Zirconium Dioxide with Abrasive Brushing Tools. *Machines* **2022**, *8*, 89. [CrossRef]
8. Uhlmann, E.; Hoyer, A. Modeling of Contact Forces for Brushing Tools. *Ceramics* **2021**, *4*, 397–407. [CrossRef]
9. Uhlmann, E.; Hoyer, A. Modellierung des Kontaktimpulses beim Bürstspanen. *Werkstattstech. Online* **2021**, *7/8*, 513–519. [CrossRef]
10. Przyklenk, K. Bestimmung des Bürstenverhaltens anhand einer Einzelborste. In *Berichte aus dem Fraunhofer-Institut für Produktionstechnik und Automatisierung (IPA), Stuttgart, Fraunhofer-Institut für Arbeitswirtschaft und Organisation (IAO), Stuttgart und Institut für Industrielle Fertigung und Fabrikbetrieb der Universität Stuttgart Nr. 87*; Warnecke, H.J., Bullinger, H.-J., Eds.; Springer: Berlin/Heidelberg, Germany, 1985.
11. Hmaidouch, R.; Müller, W.-D.; Lauer, H.-C.; Weigl, P. Surface roughness of zirconia for full-contour crowns after clinically simulated grinding and polishing. *Int. J. Oral Sci.* **2014**, *6*, 241–246. [CrossRef] [PubMed]

12. Guarnieri, R.; Miccoli, G.; Reda, R.; Mazzoni, A.; Di Nardo, D.; Testarelli, L. Sulcus fluid volume, IL-6, and Il-1b concentrations in periodontal and peri-implant tissues comparing machined and laser-microtextured collar/abutment surfaces during 12 weeks of healing: A split-mouth RCT. *Clin. Oral Implant. Res.* **2022**, *33*, 94–104. [CrossRef] [PubMed]
13. Guarnieri, R.; Zanza, A.; D'Angelo, M.; Di Nardo, D.; Del Giudice, A.; Mazzoni, A.; Reda, R.; Testarelli, L. Correlation between Peri-Implant Marginal Bone Loss Progression and Peri-Implant Sulcular Fluid Levels of Metalloproteinase-8. *J. Pers. Med.* **2022**, *12*, 58. [CrossRef] [PubMed]
14. Chieko, Y.; Armani, P.J.O. Influence of Y_2O_3 Addition on the Microstructure and Mechanical Properties of Mg-PSZ Ceramics. *JMSE* **2011**, *A1*, 556–561.
15. Lima, E.D.; Meira, J.B.C.; Özcan, M.; Cesar, P.F. Chipping of Veneering Ceramics in Zirconium Dioxide Fixed Dental Prosthesis. *Curr. Oral Health Rep.* **2015**, *2*, 169–173. [CrossRef]
16. Forkas-Tsentzeratos, G. Influence of the Surface and Heat Treatment on the Flexural Strength and Reliability of Y-TZP Dental Ceramic. Ph.D. Thesis, Medicinal Faculty of the Eberhard Karls University, Tübingen, Germany, 2010.
17. Hao, L.; Lawrence, J.; Chian, K.S. Osteoblast Cell Adhesion on a Laser Modified Zirconia Based Bioceramic. *J. Mater. Sci. Mater. Med.* **2005**, *16*, 719–726. [CrossRef]
18. Kirmali, O.; Kustarci, A.; Kapdan, A. Surface roughness and morphologic changes of zirconia: Effect of different surface treatment. *Niger. J. Clin. Pract.* **2015**, *18*, 124–129. [CrossRef]
19. Li, M.; Huang, Z.; Dong, T.; Tang, C.; Lyu, B.; Yuan, J. Surface quality of Zirconia (ZrO_2) Parts in shear-thickening high-efficiency polishing. *CIRP* **2018**, *77*, 143–146. [CrossRef]
20. Nakonieczny, D.S.; Sambok, A.; Antonowicz, M.; Basiaga, M.; Paszenda, Z.K.; Krawczyk, C.; Ziębowicz, B.; Lemcke, H.; Kałużyński, P. Ageing of Zirconia Dedicated to Dental Prostheses for Bruxers Part 2: Influence of Heat Treatment for Surface Morphology, Phase Composition and Mechanical Properties. *Rev. Adv. Mater. Sci.* **2019**, *58*, 218–225. [CrossRef]
21. Jabbar, M.K.; Dulaimi, S.F. Effect of the combined zirconium dioxide surface treatment on the shear bond strength of a veneering ceramic to zirconium dioxide. *Dent. Med. Probl.* **2020**, *57*, 177–183. [CrossRef]
22. Hoyer, A.; Uhlmann, E. Dynamik beim Bürstspanen. *Werkstattstech. Online* **2020**, *110*, 478–484. [CrossRef]